

Representation of Non-Erodible (Hard) Bottoms in Beach Profile Change Modeling

Magnus Larson[†] and Nicholas C. Kraus[‡]

[†]Department of Water
Resources Engineering
University of Lund
Box 118
S-221 00 Lund
Sweden

[‡]U.S. Army Engineer
Waterways Experiment
Station
Coastal and Hydraulics
Laboratory
3909 Halls Ferry Road
Vicksburg, MS 39180, U.S.A.

ABSTRACT

LARSON, M. and KRAUS, N.C., 2000. Representation of non-erodible (hard) bottoms in beach profile change modeling. *Journal of Coastal Research*, 16(1), 1-14. Royal Palm Beach (Florida), ISSN 0749-0208.

Non-erodible or "hard" bottoms are encountered on beaches along many coasts and are often considered a valuable environmental resource that must be protected. Hard bottoms can consist of natural materials such as limestone, coral, shell, worm rock, sedimentary rock, and clay, as well as anthropogenic materials such as rip rap. A hard bottom may be covered or uncovered by sand at various times during a storm, and it imposes a constraint on the sand transport rate. In this study, the SBEACH numerical model was modified to allow calculation of the response to storm waves and change in water level of a sand beach profile with arbitrary configurations of hard bottom. Predictions of the model were compared with one data set from a large wave tank and with several data sets from mid-scale physical model runs. The modified SBEACH model performed well both qualitatively and quantitatively in reproducing the resultant beach profile change in the presence of hard bottom for both monochromatic and random waves. A "scour attenuation coefficient" was introduced to limit unreasonable scour adjacent to vertical or near-vertical side walls of a hard bottom. To numerically simulate the mid-scale physical model runs, a scaling analysis was performed to determine the appropriate values of empirical coefficients in the numerical model. The dimensionless fall speed parameter emerged as the scaling law governing storm-induced beach profile change. Success in numerically simulating the beach-profile change measured in the mid-scale runs provides indirect evidence of the appropriateness of the governing equations of SBEACH in representing the salient physics of storm-induced beach erosion.

ADDITIONAL INDEX WORDS: *Hard bottoms, beach profile change, cross-shore sediment transport, seawall, revetment, scaling, numerical model, laboratory experiment.*

INTRODUCTION

Modern design of beach and dune complexes for storm protection normally requires application of a numerical model of beach erosion to evaluate the level of protection afforded by design alternatives (e.g., KRIEBEL and DEAN 1985; KRIEBEL 1986; LARSON and KRAUS 1989, 1991; STEETZEL, 1990; NAIRN and SOUTHGATE, 1993; ZHENG and DEAN, 1997). Along many coasts, various forms of hard bottom exist which pose challenges for such modeling and for incorporation and protection of the hard bottom itself in the design. A hard bottom is a non-erodible bottom feature that may be located anywhere on the subaerial and subaqueous beach. Hard bottom is encountered in a wide range of environments from the coral reefs in the South Pacific to cohesive shores in the Great Lakes. (Strictly speaking, a cohesive bottom will erode, although more slowly than fine clastic sediments, such as sand.) Various forms and types of hard bottom are commonly encountered along the north-central Atlantic Ocean coast of Florida, where beach nourishment is popular. Hard bottom may consist of natural materials such as worm rock, lime-

stone, coquina, coral reefs, sedimentary rocks, as well as artificial structures such as dumped concrete and rubble. Hard bottom provides habitat for marine life and is, therefore, considered to be a resource that must be protected. Natural processes such as cross-shore and longshore sand movement can cover and uncover hard bottom, but quantitative predictive tools to account for hard bottom in engineering design of beach fills and offshore mounds have not been available.

Figure 1 is an aerial photograph showing exposed hard bottom in the clear nearshore water off Martin County Beach Park, at Bathtub Reef, Florida. The hard bottom appears as at least three linear strips oriented approximately with the trend of the shoreline (the hard bottom is dark). It is expected that the narrow sand strips lying between the hard bottom plateaus are only veneers of sand temporarily trapped between them. Alternatively, sand patches may reside and move over a continuous hard bottom substrata (R. DAVIS, JR., University of South Florida, personal communication). Qualitative observation indicates that sand moves on and off such hard bottom areas according to the prevailing wave conditions. Figures 2 and 3 are ground-level photographs taken at Bathtub Reef. The hard bottom shown is built by "honeycomb" (sabellariid) worms (*phragmatopoma caudata*) that





Figure 1. Aerial view of nearshore at Martin County Beach Park at Bathtub Reef showing three bands of hard bottom.

gather sand particles and shell fragments and bind them with protein-based secretions. The voids among these living rocks provide habitat for numerous juvenile and adult organisms. In addition to hard bottom exposed on the foreshore at this beach, a substantial outcrop exists on the upper beach that developed during a geologic period of higher standing water. Such massive outcrops function as a seawall in protecting the shore by not allowing the upland to erode.

The purpose of this paper is to present a method for calculating beach profile change including non-erodible bottom areas. The presence of hard bottom alters the calculation of beach morphology change in several ways. First, and most

obvious, is that hard bottom will restrict sand movement because the area it occupies does not contribute to the sediment budget. Calculations performed as if the hard bottom were not there could indicate erosion of beach faces and dunes that cannot, in fact, erode. Such calculations might also suggest an unrealistic supply of sand to the offshore (that might cover other hard bottom areas). Designers may need to know if hard bottom will be covered by cross-shore movement of sand. If hard bottom is predicted to be covered by sand from a beach nourishment project, mitigation measures might be taken or an alternative design considered. The expected duration of coverage of hard bottom by sand brought to the area natu-



Figure 2. Ground view of worm rock on foreshore and upper beach at Bathtub Reef.

rally or through renourishment also enters in estimating environmental impacts.

CALCULATION PROCEDURE

The most obvious functioning of a non-erodible (hard) bottom is to prevent a lowering of the beach profile in locations where the hard bottom is exposed. Buried hard bottom does not alter the sand transport and profile evolution until it becomes exposed. In this respect, hard bottom functions comparably for profile evolution as does a seawall for the shoreline response produced by gradients in longshore transport. Thus, the algorithm discussed here to represent the effect of exposed hard bottom on profile response use that presented by HANSON and KRAUS (1986) for representing seawalls in shoreline change models as a starting point. NAIRN and RIDDELL (1992) and NAIRN and SOUTHGATE (1993) presented simulation results obtained with a profile response model that involved situations where a non-erodible bottom was exposed. No details were given on the algorithm employed, and it is difficult to assess the generality of their approach, such as, for example, whether the algorithm functions if the transport direction changes at arbitrary locations along the beach profile and if it conserves sand volume.

The hard bottom algorithm developed in this study accommodates complex net cross-shore transport rate distributions having several onshore and offshore peaks, as well as any number of hard bottom areas located arbitrarily across the profile. The algorithm may be incorporated in any profile response model that computes the net transport rate distribu-

tion, because the algorithm describing the constraint that the hard bottom imposes on the transport rate does not depend on how this rate is calculated. Additional information to that provided here may be found in LARSON and KRAUS (1998).

For use in coastal engineering design studies, the hard bottom algorithm was implemented in SBEACH, a numerical model of storm-induced beach profile change (LARSON and KRAUS 1989, WISE *et al.*, 1996). This model was developed using data from large wave tanks involving monochromatic waves (LARSON and KRAUS, 1989) and then validated with field data and refined to describe profile change under random waves (WISE *et al.*, 1996). SBEACH is routinely being used by the U.S. Army Corps of Engineers in project design, especially regarding beach nourishment (the latest version of SBEACH was used in the hard bottom simulations discussed here). Corps projects involving hard bottom along the Florida coast and on South Pacific territories of the United States and elsewhere provided motivation for this work. As pointed out above, the hard bottom algorithm developed here may be employed in any cross-shore transport model, see for example ROELVINK and BRØKER (1993), SCHOONNESS and THERON (1995), and ZHENG and DEAN (1997). In these studies a large number of models were compared and their applicability to simulate cross-shore sediment transport and beach profile change was assessed through various objective criterion (SBEACH was included in the two latter studies).

Theory and Numerical Implementation

Discussion is limited to cross-shore sand transport, implying that longshore sand transport is either zero or uniform



Figure 3. Massive relict worm rock on upper beach at Bathtub Reef.

over the target beach profile. The potential net cross-shore transport rate q_p is first calculated at all grid points across the profile without considering the presence of a possible hard bottom. If the hard bottom is or will become exposed during the calculation time step, constraints are placed on the transport rate so that the profile elevation remains fixed along profile segments where the hard bottom is exposed (it is assumed here that the hard bottom is non-erodible). By employing the sand volume conservation equation, the calculated depth changes based on q_p will indicate where hard bottom may restrict the transport and profile change. The sand volume conservation equation is written.

$$\frac{\partial q}{\partial x} = \frac{\partial h}{\partial t} \quad (1)$$

where q is the bulk net cross-shore transport rate including sand porosity, x is the cross-shore coordinate pointing offshore, h is the profile elevation (depth) taken positive below the still-water level (SWL), and t is the time. In discretized form of an explicit solution scheme, Eq. 1 becomes,

$$h_j^{i+1} = h_j^i + \frac{\Delta t}{\Delta x} (q_{j+1}^i - q_j^i) \quad (2)$$

where Δt is the time step, Δx is the length step, i denotes the step number in time, and j denotes the grid location along the profile. In the following, the index i is omitted if all quantities are expressed at the same time step. Eq. 2 is conve-

niently solved on a staggered grid where the elevations are defined in the middle of a calculation cell and the transport rate at the boundaries.

The elevation of the hard bottom, denoted as h_b , must be known at all grid points across shore. If the calculated potential profile elevation $h_{p,j} > h_{b,j}$ at time step $i + 1$ based on $q_{p,j+1}$ and $q_{p,j}$, then correction of the transport rate is needed because the calculated profile has moved below the hard bottom. It is only if $\partial h / \partial t > 0$ that hard bottom may constrain the transport rate. (The condition $\partial h / \partial t < 0$ implies accumulation, in which case the hard bottom is assumed to have no effect, which is equivalent to $\partial q / \partial x < 0$ according to Eq. 1.) Thus, if $q_{p,j+1} < q_{p,j}$, the hard bottom will have no effect, and transport corrections are not needed unless updrift conditions influence the transport or elevation at this location. In the opposite case ($q_{p,j+1} > q_{p,j}$), the hard bottom may restrict the transport if it is exposed or if there is not enough material in the cell above the hard bottom elevation to satisfy the calculated potential depth change. The availability of a limited volume of sand ΔV_j in cell j yields the following condition on the change in transport $\Delta q_j (= q_{j+1} - q_j$, where q denotes the correct transport rate that fulfills the hard bottom constraints),

$$\Delta V_j = \Delta q_j \Delta t = (h_{b,j} - h_j) \Delta x \quad (3)$$

implying that it is only the volume of sand available between the profile elevation h_j and the hard bottom elevation $h_{b,j}$ that

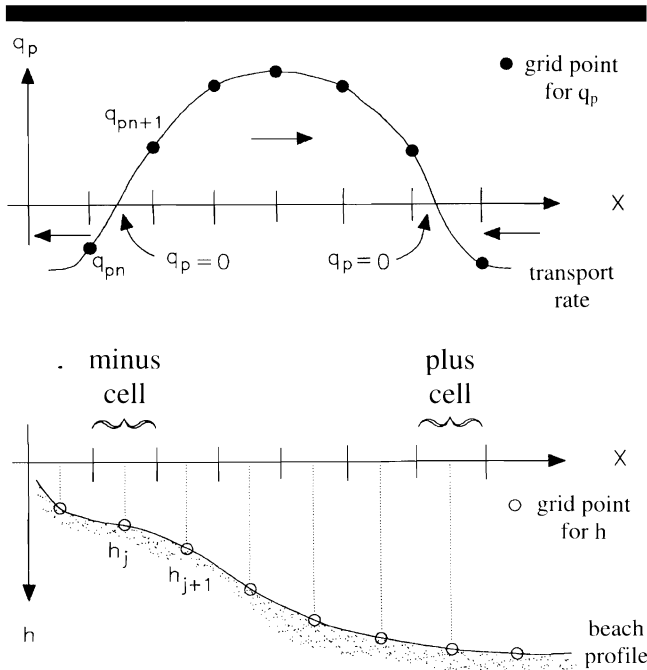


Figure 4. Schematic illustration of plus and minus cells together with grid for calculating transport rate and profile change.

is available for transport. If the hard bottom is already exposed in a particular cell, $h_j = h_{b,j}$, and $\Delta q_j = 0$.

The hard bottom can only influence points that are down-drift (in the direction of transport at a given time step) of the location where the hard bottom is exposed. An algorithm for correcting the transport rate must not only identify points where hard bottom constrains the transport, but, because the conditions at neighboring grid points are coupled through Eq. 3, restrictions imposed by up-drift-lying hard bottom must also be checked. Corrections should be made in the direction of q , and hard bottom can only influence segments along the profile where q has the same sign. Within each such segment the corrections proceed from the up-drift end to the point where the transport changes sign (or to the end of the grid, whatever is first encountered).

After computing q_p , the number and locations of segments with different transport direction (onshore or offshore) are determined. The boundaries of such transport segments are given by $q_p = 0$, and consist of either cells at the end of the grid, minus cells, or plus cells (see Figure 4; the same terminology as HANSON and KRAUS (1986) was employed). A minus cell has transport outward at both boundaries, whereas a plus cell experiences transport into it at both boundaries. Within each segment, a check is made to ascertain if hard bottom is exposed or will become exposed during a certain time step by employing the criterion $h_{p,j} > h_{b,j}$, where $h_{p,j}$ is calculated based on q_p . If this is the case, the transport is corrected starting at the up-drift end of the segment, which is a minus cell or the end of the grid, and stopping at a plus cell or the end of the grid. Along segments where the trans-

port is directed offshore, the corrections proceed toward the offshore.

If the correction of the transport rate starts in a minus cell, and the hard bottom in this cell will become exposed during a certain time step, it is not possible to uniquely determine how material is transported out of the cell. The most straightforward assumption is that the material is transported through the left and right cell boundaries in proportion to the respective potential transport rates at the boundaries (HANSON and KRAUS, 1986). In this case, the corrected transport rates may be written,

$$q_j = \frac{q_{p,j}}{q_{p,j+1} - q_{p,j}}(h_{b,j} - h_j) \frac{\Delta x}{\Delta t}$$

$$q_{j+1} = \frac{q_{p,j+1}}{q_{p,j+1} - q_{p,j}}(h_{b,j} - h_j) \frac{\Delta x}{\Delta t} \quad (4)$$

where j is the number of the minus cell (note that $q_{p,j+1} > 0$ and $q_{p,j} < 0$ for a divergence cell, so the denominator can never be zero). Eq. 4 may be manipulated to give expressions identical to those of HANSON and KRAUS (1986),

$$q_j = q_{p,j} \frac{h_{b,j} - h_j}{h_{p,j} - h_j}$$

$$q_{j+1} = q_{p,j+1} \frac{h_{b,j} - h_j}{h_{p,j} - h_j} \quad (5)$$

where $h_{p,j}$ is the potential depth at time $i + 1$ neglecting the hard bottom.

An additional check must be made directly down-drift of areas where hard bottom is exposed, because $\partial q / \partial x$ may change sign due to the hard bottom corrections. A transport gradient based on q_p may be negative, which means accumulation and no risk of hard bottom exposure; however, after corrections are made, the presence of exposed hard bottom may cause a positive gradient in q to appear down-drift of the hard bottom area. A reversal in sign of the transport gradient could happen if q_p has been reduced along the hard bottom area in order to obtain q , whereas $q = q_p$ down-drift of the area. Additional hard bottom exposure may occur that must be treated by the algorithm (for a more comprehensive discussion see LARSON and KRAUS, 1998).

Down-drift of an exposed hard bottom area, significant scour can appear if h_b increases with a sharp gradient ($h_b > 0$ below SWL, as before). In reality, for a fixed set of wave and water level conditions, it is expected that such scour would only continue until some equilibrium depth is attained (HOFFMANS (1992), HOFFMANS and PILARCZYK (1995); see also, LARSON and KRAUS (1995) for discussion of range of change in profile elevation), after which there would be no further local erosion. The model might not properly describe this situation and could overestimate the scour depending on the hard bottom configuration. A simple means of limiting the scour down-drift of hard bottom was introduced in the hard bottom algorithm. It is assumed that the transport rate increases exponentially with distance down-drift of the hard bottom to the potential value q_p , where the spatial rate of increase is determined by an empirical parameter λ_{h_b} , called

the scour attenuation coefficient. The expression used in the algorithm is,

$$q = q_p + (q_{hb} - q_p)e^{-\lambda_{hb}(x - x_{hb})} \quad x \geq x_{hb} \quad (6)$$

where q_{hb} is the transport rate at x_{hb} . Eq. 6 yields $q = q_{hb}$ if $x = x_{hb}$, and $q = q_p$ as $x \rightarrow \infty$. A larger value of λ_{hb} allows a more pronounced scour hole to develop than a smaller value. A value of $\lambda_{hb} = 1.0 \text{ m}^{-1}$ was initially implemented for evaluation, but this value must be examined in the future based on experience with the model and validation with field and laboratory measurements.

Sample Calculations with the Hard Bottom Algorithm

Sample calculations were performed for hypothetical transport rate distributions and profile and hard bottom configurations to test and evaluate the properties of the basic hard bottom algorithm. These calculations were made in a stand-alone program to more easily analyze the performance of the hard bottom algorithm and to allow testing of complex situations. The results from selected sample calculations are presented in the following to illustrate how the hard bottom algorithm operates.

An equilibrium profile was selected as the initial profile that was identical to the profile described by KRAUS and SMITH (1994) in SUPERTANK Test ST.10. The hard bottom elevations were given at all points across shore, and hard bottom was exposed along certain portions of the profile. A potential net cross-shore transport rate distribution was applied that was formed as a sum of Gaussian curves, each one with a specified standard deviation and mean, and with a maximum value that was plus (offshore) one or minus (on-shore) one. The sand conservation equation (Eq. 1) was then employed together with the hard bottom algorithm to compute the profile change resulting from the applied potential transport rate distribution. The duration of the calculation was selected so as to produce a reasonable amount of profile change. In the presented calculation results, the values of the input parameters are not of importance; focus is on the reasonability of the qualitative profile response when employing the hard bottom algorithm.

Figures 5a and 5b display the calculation results for a potential transport rate distribution with one positive (offshore-directed transport) peak and with initially exposed hard bottom between 15 and 25 m. The hard bottom was made to slope downward at 1V:5H on both sides of the exposed hard bottom. Figure 5a shows the calculated profile change, with erosion in the nearshore and deposition in the offshore where a bar-like feature is formed. The hard bottom prevents lowering of the profile in areas where it has become exposed. Additional hard bottom has been exposed compared to the initial profile because a scour hole formed downdrift of the initially exposed hard bottom. The scour attenuation coefficient λ_{hb} was set to 1.0 m^{-1} in the calculations to produce what were considered to be reasonable qualitative results; appropriate values of this parameter should be determined by comparison to measurements (see further discussion next section).

The potential transport rate q_p and the corrected transport

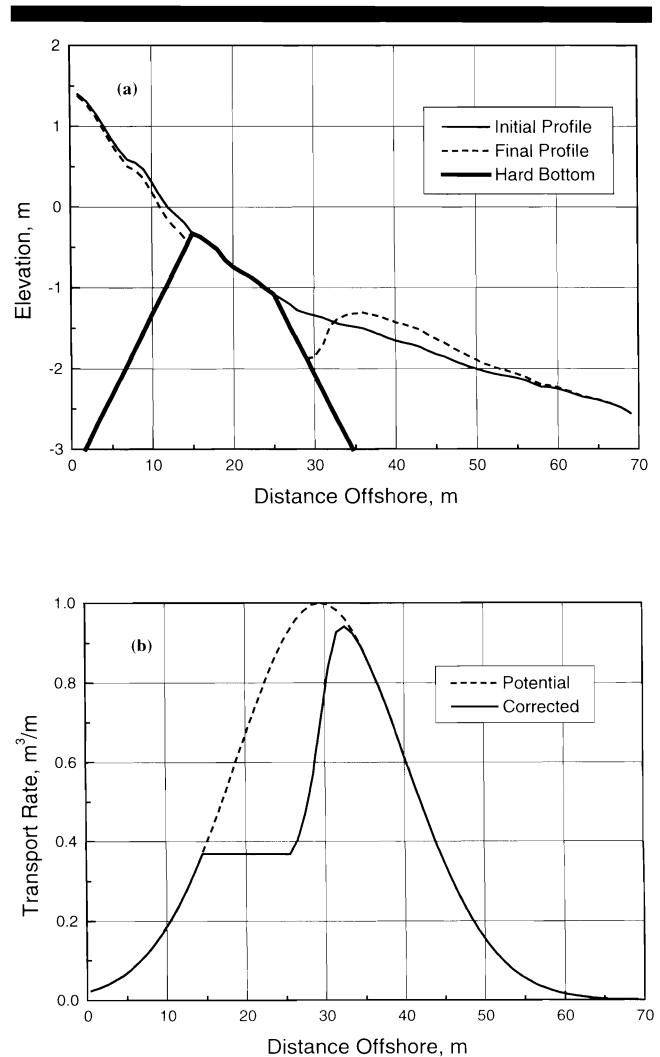


Figure 5. Sample calculation using the hard bottom algorithm showing (a) profile change around hard bottom, and (b) the potential and corrected transport rate.

rate q that fulfills the hard bottom constraint are illustrated in Figure 5b. The Gaussian-shaped q_p yields erosion in the nearshore because $\partial q_p / \partial x > 0$; however, in the area where the hard bottom is exposed no material is available to sustain this erosion; the transport coming from the updrift side of the hard bottom cannot increase, and the transported material simply passes along the exposed hard bottom. Downdrift of the hard bottom area, q increases to approach q_p because sand is available to maintain the potential transport. However, the growth in q is gradual, mainly because additional hard bottom is becoming exposed and the amount of sand available on top of the hard bottom is limited, although λ_{hb} also affects the spatial change in q .

The empirical parameter λ_{hb} , which controls how far downdrift of exposed hard bottom q_p is fully attained, influences the profile evolution mainly for configurations where the hard bottom slope is steep downdrift of an exposed section. To evaluate sensitivity of predictions to this parameter, sam-

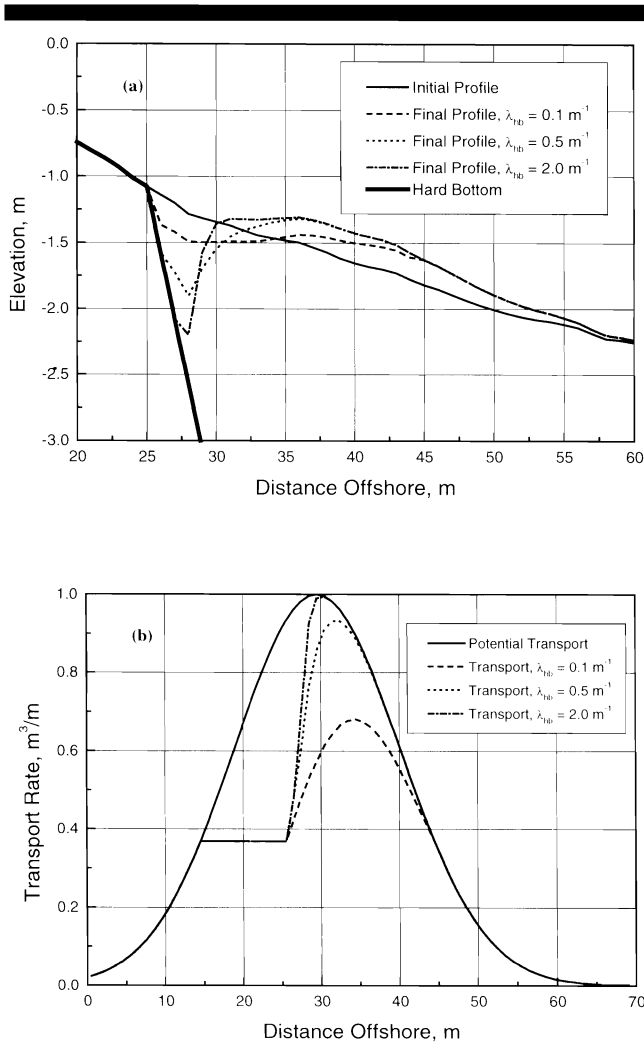


Figure 6. The effect of changing the scour attenuation coefficient λ_{hb} on (a) the profile shape, and (b) the transport correction.

ple calculations were performed for different values on λ_{hb} using the same test case as shown in Figures 6a and 6b, but with a hard bottom that sloped off at 1V:2H away from the initially exposed hard bottom area. Figures 6a and 6b display the result of changing λ_{hb} on the profile evolution directly downdrift the hard bottom area and on the transport rate, respectively.

The effective range of λ_{hb} on the profile response is limited for the values selected (Figure 6a is an enlargement of the area at the downdrift end of the hard bottom area). A value of $\lambda_{hb} = 2.0 \text{ m}^{-1}$ produces profile response that is similar to the case with no exponential transition towards q_p (or $\lambda_{hb} \rightarrow \infty$), implying development of a large scour hole. Smaller values of λ_{hb} still produce a distinct scour hole, but with a shape and depth that appear more realistic than for larger values (HOFFMANS 1992, HOFFMANS and PILARCZYK 1995). The accumulation area (bar) directly downstream of the scour hole is controlled by the value of λ_{hb} , but the effect remains rather local, and the downstream portion of the bar is not influ-

enced. The modification to q is shown in Figure 6b, where larger values of λ_{hb} yield a growth in q towards q_p at a steep gradient, which gives rise to the steep gradient in q and the associated marked scour hole.

COMPARISONS TO PHYSICAL MODEL EXPERIMENTS

Field data were not available with which to check the model predictions for profile evolution around hard bottom. However, data appropriate for testing SBEACH and the hard bottom algorithm were found in prototype-scale physical model experiments performed in Germany and in smaller "mid-scale" physical model experiments conducted in the United States.

German Large Wave Tank Test

The sample calculations in the previous section showed that the hard bottom algorithm developed in this study worked satisfactorily and produced qualitatively acceptable results. However, to quantitatively evaluate the algorithm and determine appropriate values of the scour attenuation coefficient λ_{hb} (Eq. 6), data on profile evolution involving exposed hard bottom must be employed. The most suitable data set reported in the literature for testing the hard bottom calculation algorithm and SBEACH is that of DETTE and ULICZKA (1986, 1987). They performed experiments on beach profile change in a large wave tank (Große Wellen Kanal or GWK) in Germany, where large waves and realistic beach change can be generated without physical model scale effects. During one experimental case, a significant portion of the sloping concrete bottom underlying the sand in the tank was exposed, restricting the supply of material. The sloping cement bottom was emplaced to reduce the amount of sand needed to form the beach. Exposure of the cement bottom in one fortuitous run provides measurements for evaluating the hard bottom algorithm.

The GWK is 324 m long, 7 m deep, and 5 m wide (DETTE and ULICZKA, 1986). In the case of interest, a dune without foreshore was emplaced in the tank with a seaward slope of 1V:4H from an elevation of 2 m above the SWL to the bottom of the tank located 5 m below SWL. The sand had a median grain size of $D_{50} = 0.33 \text{ mm}$, and the beach was subjected to monochromatic waves with a height $H = 1.5 \text{ m}$ and a period $T = 6.0 \text{ sec}$. These wave and sediment properties produced a markedly erosive condition, and the wave action rapidly removed material from the dune and deposited it in the offshore. After an experimental duration of less than 200 waves, so much sand had been eroded from the dune that the sloping fixed cement bottom behind the dune was exposed, limiting further profile retreat in that area. This fixed bottom also had a slope 1V:4H as did the initial dune slope, and the result of exposure of the hard bottom on profile evolution became similar to that expected on a sloping revetment.

Initially, SBEACH was run with default values of all calibration coefficients as determined from previous use of the model to other large wave tank (LWT) data (LARSON and KRAUS, 1989; LARSON *et al.*, 1990) and to field data (WISE *et al.*, 1996). The main calibration parameter is the coefficient

K in the sand transport rate equation (LARSON and KRAUS 1989); a larger value of K implies a more rapid response of the profile to the incident waves. Two other coefficients are available to modify the calculated profile response, namely, the coefficient for the slope-dependent transport ϵ and the coefficient λ that describes the decay of the transport seaward of the break point. The coefficient λ depends upon the grain size and breaking wave height (LARSON and KRAUS 1989), and its magnitude may be controlled by an empirical multiplier C_λ .

The use of the default value of K ($= 1.75 \cdot 10^{-6} \text{ m}^4/\text{N}$) produced profile evolution that was somewhat slow as compared to the GWK measurements, and K was increased to improve the agreement. A value of $K = 2.5 \cdot 10^{-6} \text{ m}^4/\text{N}$ produced satisfactory agreement. The more rapid profile change occurring in the physical model may be an artifact of the steep initial slope of the beach, which is unrealistic. The other coefficients were given the values $\epsilon = 0.001 \text{ m}^2/\text{sec}$ and $\lambda = 0.25 \text{ m}^{-1}$, which are somewhat smaller than the default values (see WISE *et al.* 1996). The hard bottom algorithm involves the scour attenuation coefficient λ_{hb} , and a value of 0.2 m^{-1} was selected mainly based on experience with the idealized simulations. Because the fixed bottom in the GWK case had a rather gentle slope for a hard bottom "side," varying λ_{hb} did not markedly alter the calculation result; thus, the GWK test is not an adequate physical situation for determining an optimal value on λ_{hb} . The GWK data do provide a severe test for a profile response model because of the steep slope of the initial profile. NAIRN and RIDDELL (1992), who performed simulations with a profile change model for a physical model case from HUGHES and FOWLER (1990) (discussed in the next section), which had a similar initial steep slope, did not start their calculations from the initial profile but substituted a profile surveyed at later times in the experiment. A more mildly sloping initial profile was probably specified to avoid instabilities in the simulations (SBEACH did not suffer this problem).

Figure 7 a–d display the initial, calculated, and measured profiles together with the location of the hard bottom (sloping fixed bottom) after 40, 370, 750, and 1,750 waves, respectively. The measured profile after 40 waves (4 min) displays a feature around the location $x = 25 \text{ m}$ that is not predicted by the model; this feature is most likely the result of initial collapse of the steep dune face as it was attacked by the waves. SBEACH partially accounts for this type of profile change through its avalanching algorithm. The profile retreat above SWL is fairly well predicted after 40 waves, although there is a short lag in the calculated profile response. The lag is more evident in Figure 7b (profile after 370 waves or 37 min), where the measured profile shows that the erosion had then reached the fixed bottom; in the calculated profile the fixed bottom is still covered with sand.

The measured bar-like feature in the offshore does not appear in the calculated profile, which has a monotonically decreasing shape in the offshore. Overall, the steeply sloping profile prevents development of a bar in the calculations. The linear shape of the profile in the offshore is a result of avalanching occurring in the beginning of the calculations. Initially, large seaward transport causes erosion

and excess steepening of the inshore part of the profile, which in turn initiates avalanching. Because of the steep initial slope avalanching can proceed to the offshore giving the profile a linear shape in this region. The small hump of sand in Figure 7b at the top of the dune appearing in the calculations is produced by overtopping (KRAUS and WISE, 1993; WISE, *et al.* 1996); the measurements indicate the presence of a similar feature.

In Figures 7c and 7d, the calculated profiles have retreated enough to expose the fixed bottom. The calculations still produce less erosion than measured, but the difference is smaller than at earlier times. Also, after 1,750 waves (175 min; Figure 7d) a small feature developed in the proper location, although it is not as pronounced as in the physical model. The calculated profile in Figure 7d is close to the equilibrium shape; therefore, a longer simulation time will only cause marginally more erosion and bar build-up. The measured profile at the end of the experiment is also close to equilibrium, which may be shown by comparing the profiles after 1,650 and 1,750 waves (not included here).

The SBEACH simulations for the GWK data involving exposure of fixed bottom show that the hard bottom algorithm can realistically simulate the constraint exerted by hard bottom on profile evolution. As a measure of the goodness of fit, the root-mean-square (rms) deviation between the measured and simulated profiles (Δh_{rms}) was calculated for each profile comparison. The computed deviations for the profiles in Figures 7a–d were $\Delta h_{rms} = 0.44, 0.36, 0.34,$ and 0.30 m , respectively, which was judged as acceptable considering the large changes that took place during the test (the rms value for the total measured change with respect to the initial profile was in the range 1.0–1.2 m for the simulation times shown in Figure 7). Thus, the deviation between measurements and simulations decreased with time elapsed. This discrepancy in the initial time response is mainly attributed to difficulties in accurately calculating the transport rate for the steep initial dune profile. A comparison between the final calculated and measured profile (close to equilibrium) supports the applicability of the hard bottom algorithm for accurately predicting how a hard bottom may limit the supply of material for transport.

Scale-Dependence of SBEACH Empirical Coefficients

Although the simulation results shown in the previous section displayed satisfactory agreement with the measurements, it was desirable to validate the algorithm for other conditions. HUGHES and FOWLER (1990) performed mid-scale physical model experiments on beach profile evolution under various combinations of sloping revetments and seawalls. This data set is suitable for further testing of the hard bottom algorithm if the physical model scale for SBEACH is resolved. Also, because beach profile change in the physical model was studied for both monochromatic and random waves, the data set provides an excellent opportunity for testing the monochromatic and random version of SBEACH together with the hard bottom algorithm.

Although the governing equations in SBEACH are based

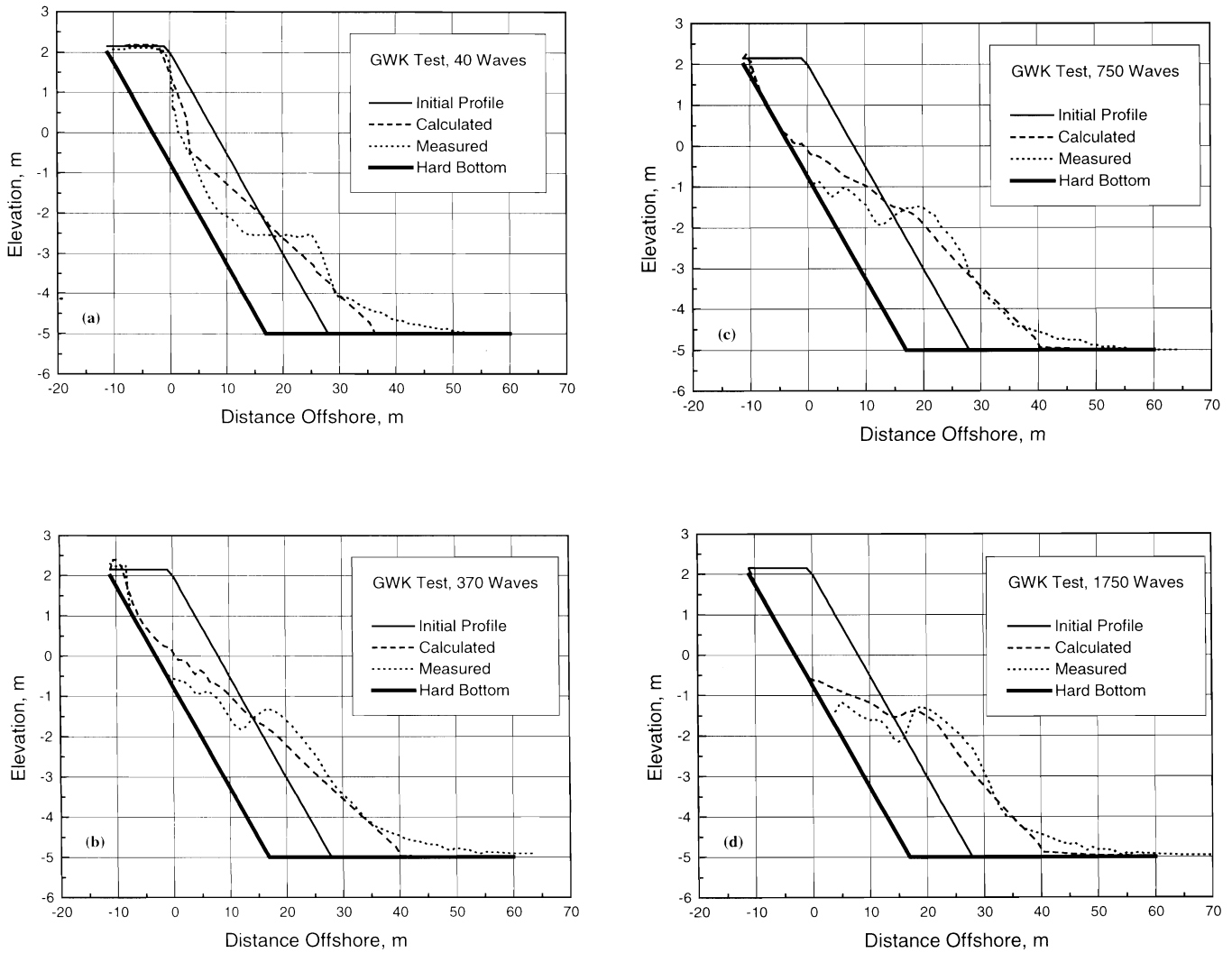


Figure 7. Calculated profiles with best-fit coefficients together with measured profiles after (a) 40, (b) 370, (c) 750, and (d) 1750 waves for the case of Dette and Uliczka (1986).

on physical principles (compare BRUUN, 1954 and DEAN, 1977), some equations were heuristically derived and include empirical coefficients. The values of these coefficients were determined based on LWT data and field data, and some of the coefficients effectively act as calibration parameters (for example, K). SBEACH has not been previously applied to laboratory-scale data and, because some of the empirical coefficients are dimensional, the typical ranges of values found valid for the field are not expected to apply at smaller scale. Thus, a simplified set of the governing equations in SBEACH was studied as described next to determine scaling laws for the leading empirical coefficient, K . ZHENG and DEAN (1997) also discussed a similar transport coefficient and how to establish values independent of scale.

The wave transformation (DALLY *et al.*, 1985), net cross-shore transport rate, and beach change may be calculated, respectively, with the following equations,

$$\frac{dF}{dx} = \frac{\kappa}{d}(F - F_{st}) \tag{7}$$

$$\frac{\partial q}{\partial x} = \frac{\partial h}{\partial t} \tag{8}$$

$$q = K(D - D_{eq}) \tag{9}$$

where F is the wave energy flux and F_{st} is the corresponding stable value, D is the wave energy dissipation per unit water volume ($= 1/d \, dF/dx$), D_{eq} is the corresponding equilibrium value, d is the total water depth, and κ is an empirical coefficient. Eqs. 7–9 constitute a simplification of the governing equations in SBEACH; representation of the physics contained in the model is still captured by the equations. For shallow water, the wave energy flux is,

$$F = \frac{1}{8} \rho g H^2 \sqrt{gd} \tag{10}$$

where ρ is the density of water, g is the acceleration of gravity, and H is the wave height. At stable conditions (no further breaking or wave height decay), the wave height is given by $H_{st} = \Gamma d$, where Γ is a non-dimensional empirical coefficient, and H_{st} may be substituted in Eq. 10 to obtain F_{st} .

To proceed in the scaling analysis, length is normalized with a representative wave height H_l and time is normalized with a representative wave period T_l in Eqs. 7–9. The normalization leads to the non-dimensional equations,

$$\frac{dF'}{dx'} = \frac{\kappa}{d'}(F' - F'_s) \quad (11)$$

$$q' = \frac{1}{d'} \frac{dF'}{dx'} - D'_{eq} \quad (12)$$

$$\frac{1}{8} \frac{\rho g^{3/2} K T_l}{H_l^{3/2}} \frac{\partial q'}{\partial x'} = \frac{\partial h'}{\partial t'} \quad (13)$$

where a prime denotes a non-dimensional quantity, and:

$$D'_{eq} = \frac{D_{eq}}{\frac{1}{8} \rho g \sqrt{g H_l}} \quad (14)$$

Thus, if the following conditions hold,

$$\frac{1}{8} \frac{\rho g^{3/2} K T_l}{H_l^{3/2}} = \text{Constant} \quad (15)$$

$$\frac{D_{eq}}{\frac{1}{8} \rho g \sqrt{g H_l}} = \text{Constant} \quad (16)$$

the equations will predict an identical non-dimensional profile evolution in time $h'(x', t')$, where $h' = h/H_l$, $x' = x/H_l$, and $t' = t/T_l$.

Recognizing that ρ and g are constants, Eqs. 15 and 16 yield two scaling conditions which, when applied to two situations numbered as 1 and 2 give:

$$\left(\frac{K T_l}{H_l^{3/2}} \right)_1 = \left(\frac{K T_l}{H_l^{3/2}} \right)_2 \quad (17)$$

$$\left(\frac{D_{eq}}{\sqrt{H_l}} \right)_1 = \left(\frac{D_{eq}}{\sqrt{H_l}} \right)_2 \quad (18)$$

KRIEBEL *et al.* (1991) showed based on data that D_{eq} is directly proportional to the sediment fall speed w , and Eq. 18 may therefore be rewritten:

$$\left(\frac{w}{\sqrt{H_l}} \right)_1 = \left(\frac{w}{\sqrt{H_l}} \right)_2 \quad (19)$$

Retaining the g inside the square-root sign of the denominator in Eq. 19 produces a non-dimensional parameter discussed by KRAUS *et al.* (1991) (see also DALRYMPLE, 1992) for distinguishing erosional and accretionary events on a beach. Furthermore, under the assumption that K is constant for Conditions 1 and 2, Eqs. 17 and 19 may be combined to yield to the condition that the non-dimensional fall speed H_l/wT_l should be constant.

As expected, preliminary simulations with SBEACH for the

mid-scale data using default values over-predicted the speed of erosion. Thus, the conclusion is that K (and some of the other dimensional coefficients) is influenced by scale and, before applying SBEACH to smaller scale laboratory experiments, some adjustment is needed. An adjustment is, perhaps, *a priori* evident because K is a dimensional empirical coefficient.

As an indication on the relationship between K at prototype and model scale, Eq. 17 gives the following.

$$\frac{K_p}{K_m} = \left(\frac{H_p}{H_m} \right)^{3/2} \frac{T_m}{T_p} \quad (20)$$

where the subscript p denotes prototype, and m denotes model conditions. The ratio H_p/H_m is given by the geometric scale l ; however, a scaling law has to be selected to obtain T_p/T_m , and thus K_p/K_m . The Froude modeling law (HUGHES, 1993) is often used in coastal engineering applications, which yields $T_p/T_m = l^{0.5}$. Under this assumption, Eq. 20 gives,

$$\frac{K_p}{K_m} = l \quad (21)$$

which implies that K scales in proportion to the geometric scale. Thus, before applying SBEACH to smaller scale laboratory data, K should be divided by l as the fundamental scaling law for SBEACH.

Mid-Scale Experiment Comparisons

One of the main objectives of HUGHES and FOWLER (1990) was to validate scaling laws for physical models involving cross-shore sediment transport and erosion near structures. In order to confirm the validity of the scaling laws used, HUGHES and FOWLER reproduced in a mid-scale physical model the DETTE and ULICZKA (1986) case discussed in the previous section. The sediment was scaled with the fall speed parameter H/wT , and other quantities were specified through Froude scaling.

The mid-scale experiments were done at a geometric scale of 1:7.5 (scale ratio $l = 7.5$ between prototype and model). Using the fall speed parameter to scale the grain size yielded $D_{50} = 0.13$ mm in the model. The same grain size and initial beach profile configuration (scale-copy of the DETTE and ULICZKA case; dune without foreshore sloping at 1:4, with fixed bottom having the same slope under the sand) were used in all cases, with the exception that a seawall was placed around the still-water shoreline in some tests. The duration of the runs was typically 1,850 waves during which several profile surveys were conducted. The basic wave- and water-level conditions were $H = 0.2$ m, $T = 2.2$ sec, and a total water depth $d = 0.67$ m. In the random wave tests, either the root-mean-square (rms) or the significant wave height was set equal to 0.2 m to determine the statistical wave height that gave profile evolution agreeing closest with that produced by monochromatic waves. Table 1 summarizes the HUGHES and FOWLER cases considered here (case numbering from HUGHES and FOWLER) to evaluate SBEACH and the hard bottom algorithm.

In the following, the simulation results are briefly discussed for each case. Comparisons are made for the final

Table 1. Summary of cases from HUGHES and FOWLER (1990).

Case No.	Wave and Beach Conditions
T03	Monochromatic waves, sloping revetment
T08	Random waves ($H_{rms} = H_{mono}$), sloping revetment
T09	Random waves ($H_{1/3} = H_{mono}$), sloping revetment
T10	Monochromatic waves, sloping revetment and seawall
T11	Random waves ($H_{1/3} = H_{mono}$), sloping revetment and seawall

Note: H_{rms} : rms wave height, $H_{1/3}$: significant wave height, H_{mono} : monochromatic wave height

measured profile and for one intermediate profile in the experiments. The final profile was taken after 1,850 waves had run (except in T08 where the final profile is after 1,650 waves), whereas the intermediate profile shown is that developed after 370 waves. The rms deviation (Δh_{rms}) was computed for each profile comparison, as previously described.

Case T03

This case aimed at reproducing the previously described GWK case. Monochromatic waves were allowed to attack the dune without a foreshore, and a sloping revetment was placed under the sand. Figures 8a and 8b display comparison between SBEACH calculations and the mid-scale physical model results ($\Delta h_{rms} = 0.060$ and 0.035 m, respectively). The profile retreat predicted by SBEACH is somewhat greater than the measurements after 370 waves (note the distinct measured scarp in Figure 8a), and the calculations do not show the pronounced offshore bar obtained in the physical model at this elapsed time. Also, the revetment is not yet exposed. However, after 1,850 waves the entire revetment above SWL is uncovered, which is well predicted by SBEACH; also, the model predicts a bar at a location along the profile and with similar dimensions as was measured.

Case T08

The experimental arrangement was the same as in T03, but random waves were employed with the rms wave height equal to the monochromatic wave height (implying an equal amount of wave energy for the two wave conditions). The agreement between calculations and the physical model is better than for Case T08, especially after 370 waves (Figure 9a), although the calculated profiles are smoother than the measured ($\Delta h_{rms} = 0.037$ m). The subdued bar feature occurring in the measured profile after 1,650 waves (Figure 9b) is not described by the numerical model ($\Delta h_{rms} = 0.030$ m). Comparison to Figures 8a and 8b shows the difference in profile change calculated with random waves and with monochromatic waves. The bar appearing in Figure 8b is absent in Figure 9b because of the smoothing process of the random waves.

Case T09

This case was also identical to Case T08, except that the significant height of the random waves was set equal to the monochromatic wave height, implying that the random waves in total had less total energy than the monochromatic

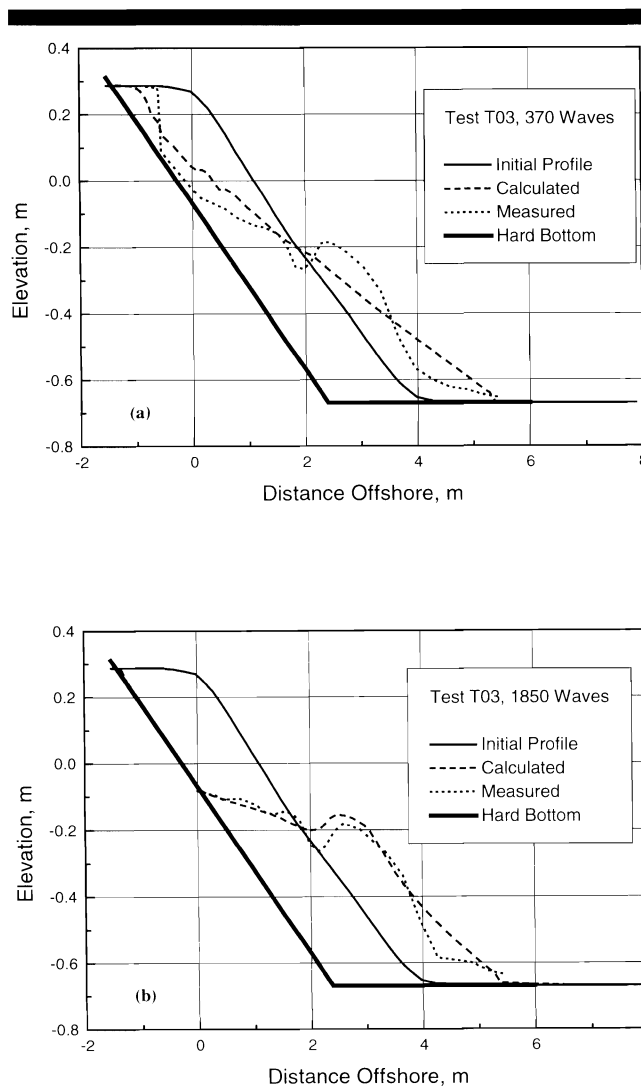


Figure 8. Calculated and measured profiles after (a) 370 and (b) 1850 waves for Case T03 of Hughes and Fowler (1990).

waves. Figures 10a and 10b illustrate the calculated profiles and the corresponding measurements ($\Delta h_{rms} = 0.055$ and 0.042 m, respectively). As in the calculations for Case T03, SBEACH predicted a profile retreat that is somewhat more rapid than the measurements. The overall agreement and the calculated exposure of the revetment is judged satisfactory.

Case T10

A seawall was placed around the still-water shoreline and covered with sand, with the sloping revetment still in place. Monochromatic waves were employed, causing the profile to retreat rapidly and uncover the seawall. Figures 11a and 11b show the calculated and measured profiles after 370 and 1,850 waves, respectively. The seawall in the physical model is completely exposed after 370 waves, whereas the sloping revetment is still covered with sand ($\Delta h_{rms} = 0.047$ m). This development is predicted well by the numerical model; as be-

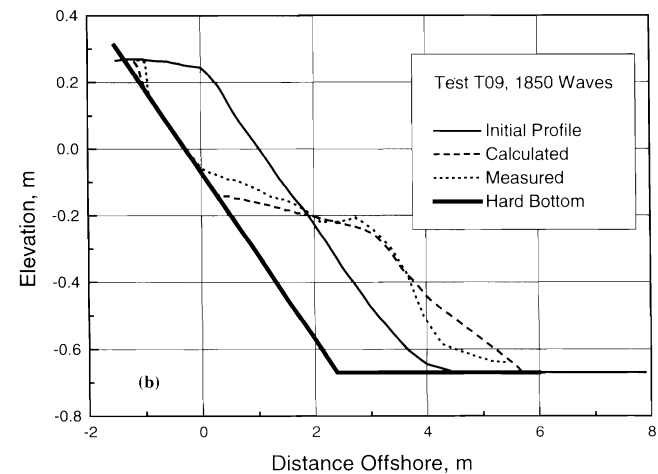
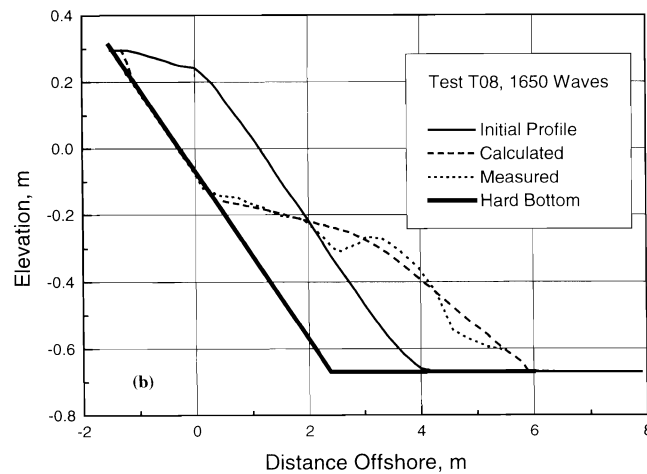
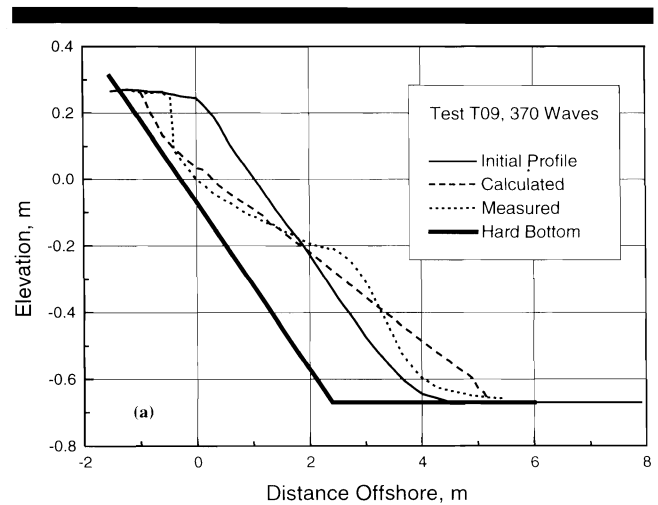
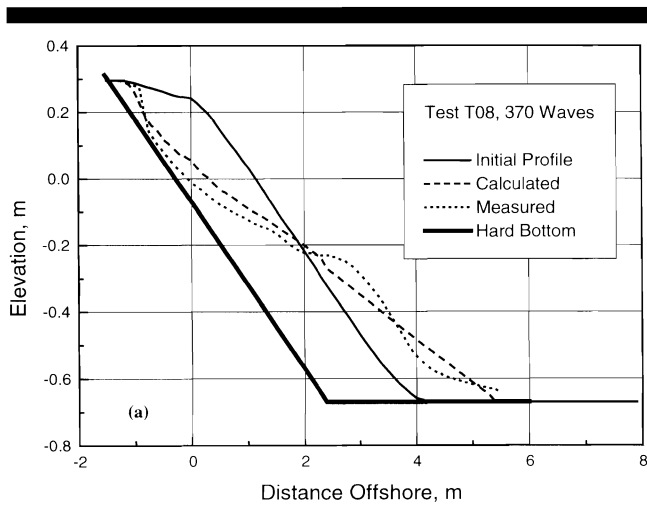


Figure 9. Calculated and measured profiles after (a) 370 and (b) 1650 waves for Case T08 of Hughes and Fowler (1990).

Figure 10. Calculated and measured profiles after (a) 370 and (b) 1850 waves for Case T09 of Hughes and Fowler (1990).

fore, the bar in the offshore does not appear in the model calculations after 370 waves. However, after 1,850 waves SBEACH produces a clear bar, although its crest is located somewhat inshore of the measured bar ($\Delta h_{rms} = 0.051$ m). The marked trough generated in the physical model shown in both Figures 11a and 11b, which may be related to reflection of the monochromatic waves from the vertical wall, is absent in the numerical model calculations.

Case T11

This case was identical to Case T10 with the exception that random waves were used, where the significant wave height was set equal to the monochromatic wave height in T10. The agreement between calculations and measurements (Figures 12a and 12b; $\Delta h_{rms} = 0.040$ and 0.032 m, respectively) is somewhat better than for the monochromatic case. A distinct bar was not formed because of the smoothing produced by

the random waves, and the trough observed in Figure 11 that may have been formed by reflected monochromatic waves is also absent in the physical model.

CONCLUDING DISCUSSION

The SBEACH model was enhanced to account for a non-erodible (hard) bottom in the calculation domain. Arbitrary numbers and locations of hard bottom can be specified. High-quality laboratory data were available for testing the newly developed hard bottom algorithm. The hard bottom implementation was evaluated in sensitivity tests for qualitatively reasonable results and was found to perform well. Comparison with a case of hard bottom exposure measured in a large wave tank and with measurements from several tests performed in a mid-scale physical model were also successful. The comparisons with the mid-scale tests also validated the

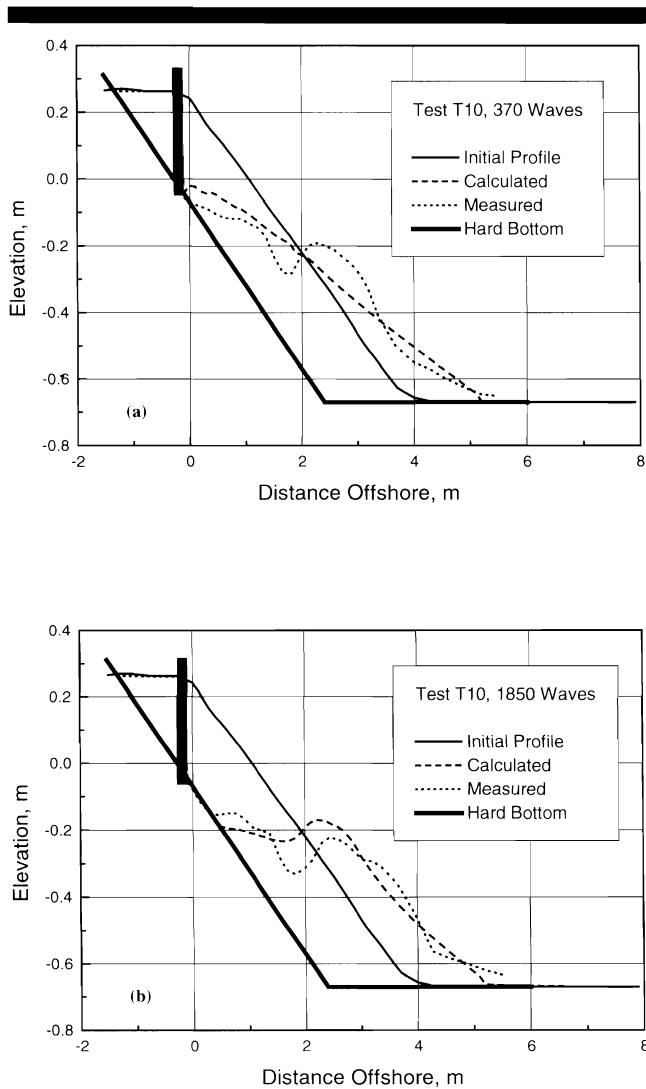


Figure 11. Calculated and measured profiles after (a) 370 and (b) 1850 waves for Case T10 of Hughes and Fowler (1990).

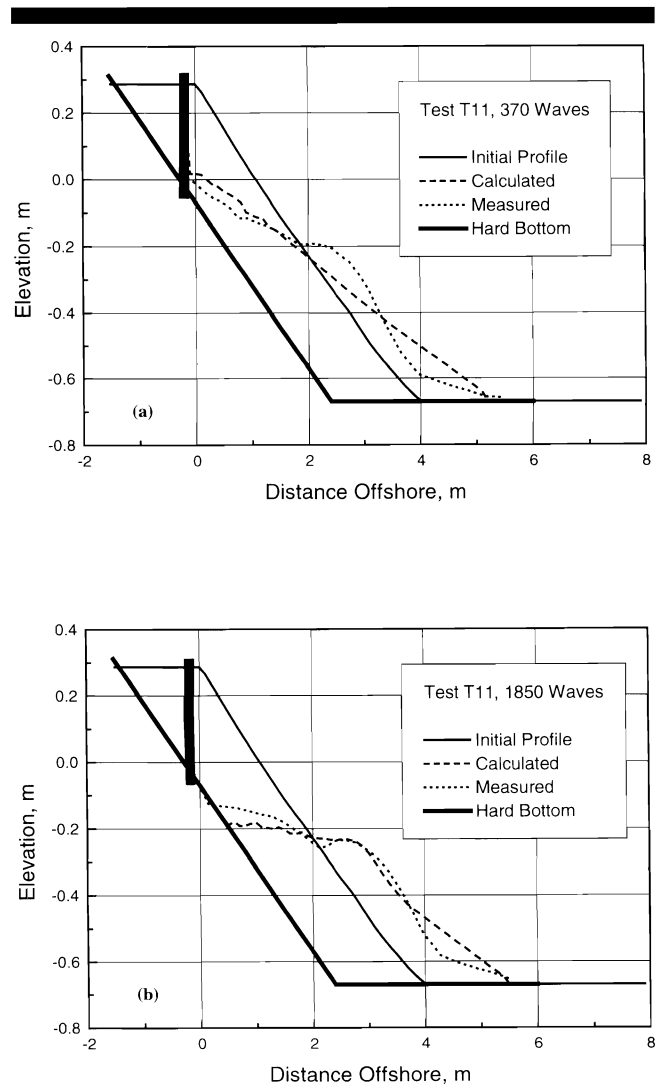


Figure 12. Calculated and measured profiles after (a) 370 and (b) 1850 waves for Case T11 of Hughes and Fowler (1990).

monochromatic and random-wave transport calculations in SBEACH.

Predictions of SBEACH produced satisfactory agreement with the measurements made in the mid-scale physical model experiments. No calibration was performed for the comparisons, with the empirical coefficient values determined for the GWK physical model comparison employed directly after appropriate scaling. SBEACH proved capable of not only giving realistic simulation results for the smaller scale experiments, but also for both monochromatic and random waves in various combinations with the shore-protection structures of sloping revetments and a seawall.

A scaling criterion was derived for applying the numerical model to simulate the mid-scale physical model tests. Success in reproducing the physical model results with SBEACH is an indirect confirmation that the basic physical principles

acting to produce storm-induced beach erosion are represented in the numerical model.

SBEACH has been shown to be applicable to calculate storm-induced beach erosion on beaches containing hard bottom areas in the nearshore. In this capacity, the model is expected to be an aid in design of beach fills and in guiding field-data collection as well as laboratory tests aimed at investigating the physical processes in the vicinity of hard bottom. Although the hard bottom algorithm developed in this study can handle cross-shore transport distributions of arbitrary shape, the presently used version of SBEACH does not include onshore transport and accretion. Thus, it remains to validate the algorithm for conditions when the sediment moves onshore and hard bottom affects the transport. However, since the algorithm is based mainly on the continuity equation and geometrical considerations, it is expected that it has a potential for working equally well for onshore transport and accretionary conditions.

ACKNOWLEDGEMENTS

This work was supported by the U.S. Army Corps of Engineers, Jacksonville District, Jacksonville, Florida. We appreciate the guidance and information provided by Mr. Peter Grace, Ms. Cynthia Perez, Mr. David Schmidt, and Mr. Thomas Smith of the Jacksonville District. Mr. Randall Wise of the U.S. Army Engineer Waterways Experiment Station, Coastal Engineering and Hydraulics Laboratory (CHL), kindly provided coordination on CHL's current version of SBEACH. We appreciate the kind cooperation of Dr. Hans Dette of the University of Braunschweig, Germany, and of Dr. Steven Hughes of CHL, for providing their data. Permission to publish this paper was granted by the Chief of Engineers, U.S. Army Corps of Engineers. Professor Robert G. Dean provided valuable review comments which is gratefully acknowledged.

LITERATURE CITED

- BRUUN, P., 1954. Coast Erosion and the Development of Beach Profiles. *Technical Memorandum No. 44*, Beach Erosion Board, U.S. Army Corps of Engineers.
- DALLY, W.R.; DEAN, R.G., and DALRYMPLE, R.A., 1985. Wave height variation across beaches of arbitrary profile. *Journal of Geophysical Research*, 90(C6), 11917–11927.
- DALRYMPLE, R.A., 1992. Prediction of storm/normal beach profiles. *Journal of Waterway, Port, Coastal, and Ocean Engineering*, 118(2), 193–200.
- DEAN, R.G., 1977. Equilibrium beach profiles: US Atlantic and Gulf Coasts. Department of Civil Engineering, *Ocean Engineering Report No. 12*. University of Delaware, Newark, Delaware.
- DETTE, H.H. and ULICZKA, K., 1986. Velocity and sediment concentration fields across surf zones. *Proceedings of the 20th Coastal Engineering Conference*, (ASCE), pp. 1,062–1,076.
- DETTE, H.H. and ULICZKA, K., 1987. Prototype investigations on time-dependent dune recession and beach erosion. *Proceedings of Coastal Sediments '87*, (ASCE), pp. 1,430–1,444.
- HANSON, H. and KRAUS, N.C., 1986. Seawall boundary condition in numerical models of shoreline evolution. *Technical Report CERC-86-3*, US Army Engineer Waterways Experiment Station, Vicksburg, Mississippi.
- HOFFMANS, G.J.C.M., 1992. Two-dimensional mathematical modeling of local-scour holes. *Report 92-7, Communications on Hydraulic and Geotechnical Engineering*, Delft University of Technology, Delft, The Netherlands.
- HOFFMANS, G.J.C.M. and PILARCZYK, K.W., 1995. Local scour downstream of hydraulic structures. *Journal of Hydraulic Engineering*, 121(4), 326–340.
- HUGHES, S.A., 1993. *Physical Models and Laboratory Techniques in Coastal Engineering*, Advanced Series on Ocean Engineering, Vol. 7. Singapore: World Scientific.
- HUGHES, S.A. and FOWLER, J.E., 1990. Mid-scale physical model validation for scour at coastal structures. *Technical Report CERC-90-8*, US Army Engineer Waterways Experiment Station, Vicksburg, Mississippi.
- KRAUS, N.C.; LARSON, M., and KRIEBEL, D.L., 1991. Evaluation of beach erosion and accretion predictors. *Proceedings of Coastal Sediments '91*, (ASCE), pp. 572–587.
- KRAUS, N.C. and SMITH, J.M., 1994. SUPERTANK laboratory data collection project. Volume I: Main text. *Technical Report CERC-94-3*, U.S. Army Engineer Waterways Experiment Station, Vicksburg, Mississippi.
- KRAUS, N.C., and WISE R.A., 1993. Simulation of January 4, 1992, storm erosion at Ocean City, Maryland. *Shore and Beach*, 61(1), 34–41.
- KRIEBEL, D.L., 1986. Verification of a dune erosion model. *Shore and Beach*, 54(3), 13–21.
- KRIEBEL, D.L. and DEAN, R.G., 1985. Numerical simulation of time dependent beach and dune erosion. *Coastal Engineering*, 9, 221–245.
- KRIEBEL, D.L.; KRAUS, N.C., and LARSON, M., 1991. Engineering methods for predicting beach profile response. *Proceedings of Coastal Sediments '91*, (ASCE), pp. 557–571.
- LARSON, M. and KRAUS, N.C., 1989. SBEACH: numerical model for simulating storm-induced beach change. Report 1: empirical foundation and model development. *Technical Report CERC-89-9*, U.S. Army Engineer Waterways Experiment Station, Vicksburg, Mississippi.
- LARSON, M. and KRAUS, N.C., 1991. Mathematical modeling of the fate of beach fill. In: H.D. Niemeier, J. van Overeem, and J. van de Graaff, (Editors), *Artificial Beach Nourishments*, Special Issue of *Coastal Engineering*, 16, 83–114.
- LARSON, M. and KRAUS, N.C., 1995. Prediction of cross-shore sediment transport at different spatial and temporal scales. *Marine Geology*, 126, 111–127.
- LARSON, M. and KRAUS, N.C., 1998. SBEACH: numerical model for simulating storm-induced beach change. Report 5: Representation of non-erodible (hard) bottoms. *Technical Report CERC-89-9*, U.S. Army Engineer Waterways Experiment Station, Vicksburg, Mississippi.
- NAIRN, R.B. and RIDDELL, K.J., 1992. Numerical beach profile modelling for beachfill projects. *Proceedings of Coastal Practice '92*, (ASCE), pp. 12–28.
- NAIRN, R.B. and SOUTHGATE, H.N., 1993. Deterministic profile modelling of nearshore processes. Part 2. sediment transport and beach profile development. *Coastal Engineering*, 19, 57–96.
- ROELVINK, J.A. and BRØKER, I., 1993. Cross-shore profile models. *Coastal Engineering*, 21, 163–191.
- SCHOONEES, J.S. and THERON, A.K., 1995. Evaluation of 10 cross-shore sediment transport/morphological models. *Coastal Engineering*, 25, 1–41.
- STEETZEL, H.J., 1990. Cross-shore transport during storm surges. *Proceedings of the 22nd Coastal Engineering Conference*, (ASCE), pp. 1,922–1,934.
- WISE, R.A.; SMITH, S.J., and LARSON, M., 1996. SBEACH: numerical model for simulating storm-induced beach change. Report 4. Cross-shore transport under random waves and model validation with SUPERTANK and field data. *Technical Report CERC-89-9*, U.S. Army Engineer Waterways Experiment Station, Vicksburg, Mississippi.
- ZHENG, J. and DEAN, R.G., 1997. Numerical model and intercomparisons of beach profile evolution. *Coastal Engineering*, 30, 169–201.